

Monopersulfate photocatalysis under 365 nm radiation. Direct oxidation and monopersulfate promoted photocatalysis of the herbicide tembotrione

Rafael R. Solís*, F. Javier Rivas, Mercedes Tierno

Department of Chemical Engineering and Physical Chemistry, University of
Extremadura, Av. Elvas s/n, 06071 Badajoz, Spain

*Correspondence to: Rafael R. Solís, Departamento de Ingeniería Química y Química Física, Universidad de Extremadura, Avda. Elvas s/n, 06071, Badajoz (Spain). Email: rrodrig@unex.es, Phone: +34924289300, Fax: +34924289385

Abstract

Oxone® (potassium monopersulfate, MPS) has been used to oxidize the herbicide tembotrione in aqueous solution. Tembotrione elimination kinetics by MPS direct oxidation has been studied. The influence of the main operating variables affecting the process (MPS concentration, temperature and pH) has been evaluated. The process follows 2/3 and first orders in MPS and tembotrione concentrations, respectively. Optimal pH is located around circumneutral conditions. MPS decomposition in the presence of 365 nm UVA radiation and titanium dioxide has also been studied. A kinetic mechanism that simulates MPS decomposition has been proposed, showing the positive effect of titania load and MPS concentration. The system MPS/UVA/TiO₂ significantly improves tembotrione and mineralization rate abatement if compared to runs conducted in the absence of MPS. Tembotrione total abatement was achieved in 20 min when 0.05 g L⁻¹ of titania and 10⁻⁴ M of Oxone® were used. TOC conversion was roughly 70% in 90 min under similar operating conditions. An experimental design (Plackett-Burman) has been considered to study the influence of the main variables affecting tembotrione photocatalytic oxidation promoted by MPS.

Key words: tembotrione, monopersulfate, oxone, photocatalysis, UVA radiation

1. INTRODUCTION

As a consequence of increasing population needs, pesticides are used in intensive farming around the world. Uncontrolled use of pesticides supposes an alarmingly hazard for the environment and human health. Triketone herbicides, such as sulcotrione, mesotrione or tembotrione, are 4-hydroxyphenylpyruvate dioxygenase (HPPD) inhibitors, which act blocking the HPPD indispensable enzyme in plant growth. Thus, the plant develops leaf bleaching followed by necrosis and death (Sutton et al., 2002). Since some weeds developed resistance to traditional herbicides and because pesticide legislation became more restrictive to classical herbicides HPPD inhibitors were brought to North American and European markets as the newest class herbicides in the late 1990s and 2000s. Tembotrione (TEMB), 2-[2-chloro-4-mesyl-3-((2,2,2-trifluoroethoxy)methyl)benzoyl]cyclohexane-1,3-dione, was launched in 2007 by Bayer CropScience (Laudis®) to control different types of grass and broadleaf weeds during the early to mid-post-emergence of field corn (Tarara et al., 2009). Although TEMB is mostly used in popcorn crop, sweet corn and seed corn fields; other applications, like in sorghum and soyabean, are still under consideration. In 2013, the global demand of the tembotrione market was 267.4 tons and it is expected to reach a market value of US\$51.2 million by 2020 (Transparency Market Research USA & Canada, 2015). Since tembotrione is one of the newest herbicides released, little is known about the effects on the environment; however, its use is currently approved in the European Union (European Union, 2012).

Pesticides, as an example of organic and emerging contaminant, are not properly removed in conventional biological wastewater treatment. Amongst the advanced oxidation processes applied to herbicides management, photocatalysis has raised a great

interest, particularly if considering the use of solar radiation which reduces the environmental impact if compared to other technologies. To the authors' knowledge, not many works have dealt with the oxidation of tembotrione in water. Although chlorination (Tawk et al., 2015), photolysis (Calvayrac et al., 2013; Trivella et al., 2015; Halle and Richard, 2006) Fenton process (Bensalah et al., 2011) and other Advanced Oxidation Processes (Jović et al., 2013; Murati et al., 2012) have been reported in the elimination of triketone herbicides, few of them include tembotrione in their research.

Oxone® is a chemical manufactured by DuPont. This compound is a triple salt (MPS, $2\text{KHSO}_5 \cdot \text{KHSO}_4 \cdot \text{K}_2\text{SO}_4$). MPS is considered an alternative to other chemical oxidants because of several advantages. It is a homogeneous oxidant whose activity is higher than other traditional oxidants like hydrogen peroxide. MPS decomposes into sulfate and hydroxyl radicals. Sulfate radicals present a higher standard reduction potential compared to hydroxyl radicals (2.5-3.1 V at neutral pH versus 1.8-2.7 V depending on the pH). Moreover, MPS decomposition is easily promoted by transition metals (Sun et al., 2009) or by heterogeneous catalysts (Anipsitakis et al., 2005; Su et al., 2013; Yao et al., 2013), UV radiation (Fernández et al., 2004; Rivas et al., 2010) or heat (Gao et al., 2015). Furthermore, MPS is usually labelled as an environmentally-friendly oxidant, as it does not generate toxic byproduct after its application. MPS research has recently been focused on the removal of phenols (Anipsitakis et al., 2006; Ji et al., 2011), pharmaceutical compounds (Rivas et al., 2013; Deng et al., 2013), herbicides (Romero et al., 2010), chlorinated compounds (Cong et al., 2015), and disinfection (Anipsitakis et al., 2008). However, to date, few works have integrated the use of MPS as oxidant promoter and photocatalysis (Malato et al., 1998; Gimeno et al., 2007; Shukla et al., 2010). Moreover, little attention has been paid to the mechanism of MPS decomposition through photocatalytic processes.

Since previous experiments revealed the direct reaction between oxone and tembotrione, in this work, this herbicide has been oxidized in the presence of MPS. The most influencing variables in the process such as MPS concentration, temperature and pH, have been studied. In order to improve mineralization extent, MPS was used as a promoter in the photocatalytic tembotrione oxidation using TiO₂. Previously, MPS decomposition under 365 nm UVA radiation has been assessed. A kinetic mechanism which acceptably simulates the process has been proposed. Finally, MPS photocatalytic oxidation of tembotrione has been studied. A Plackett-Burman experimental design has been completed to examine the weight of the main variables of the process (MPS, tembotrione concentration and catalyst load).

2. EXPERIMENTAL

2.1. Materials

Analytical standard tembotrione (PESTANAL®, CAS 335104-84-2) was purchased from Sigma-Aldrich and was used as received in all the experiments. Oxone® and the rest of chemicals were acquired from Sigma-Aldrich. Acetonitrile from VWR Chemicals was used in HPLC determination of tembotrione. All solutions were prepared with ultrapure water from a Mili-Q® academic (Millipore) system. Commercial TiO₂ Degussa P25 (70 % anatase and 30 % rutile) was the photocatalyst used in heterogeneous experiments (average particle size of 30 nm and BET surface area of 50 m² g⁻¹).

2.2. Analytical methods

Tembotrione was quantified by means of an Agilent 1100 (Hewlett-Packard) high performance liquid chromatography system with UV detection (HPLC-UV). A Kromasil 100 5C18 (5µm, 2.1x150 mm) column was connected. The mobile phase was a 50:50 (A:B) mixture of 0.1% H₃PO₄ acidified water (A) and acetonitrile (B). UV

detection was conducted at 250 nm. Relative error of HPLC determination, expressed as relative standard deviation of a sample of 5 mg L⁻¹ of tembotrione which was analyzed 10 times, was found to be 0.46%. Moreover the limit of detection of the calibration curve (Miller and Miller, 2010) was 54.5 µg L⁻¹.

Tembotrione mineralization was monitored by analyzing the total organic carbon (TOC) in a Shimadzu TOC 5000A analyzer. 1.31% of relative error was obtained (5 mg L⁻¹ of tembotrione which corresponds to 2.5 mg L⁻¹ of TOC) and the limit of detection of the calibration curve was 336 µg L⁻¹.

MPS concentration evolution was analyzed spectrophotometrically by a colorimetric method based on N,N-diethyl-p-phenylenediamine (DPD) oxidation (Fukushima and Tatsumi, 2005), with a relative error of 3.44%. pH of the reaction media was adjusted and controlled by means of a Radiometer Copenhagen pH-meter (HPM82).

2.3. Photoreactor setup and experimental procedure

The reaction system, whose scheme is depicted in Figure 1, consisted of a cylindrical 1.0 L borosilicate photoreactor. The glass reactor was located in the middle of a 31 cm external diameter pipe of 54 cm height. The reactor was magnetically stirred by an IKA® RCT basic stirrer equipped with temperature control. In order to maximize photons reflection, the internal wall of the pipe was covered by aluminum foil. Four black light lamps of 41 cm height (LAMP15TBL HQPOWER™ manufactured by Velleman®) were evenly placed and attached to the internal wall of the pipe. Each lamp, which a nominal power of 15 W, mainly emits radiation within the range 350-400 nm with a maximum located at 365 nm. UVA photon flow was determined in a previous work by means of ferrioxalate actinometry. Values of 1.77, 3.26, 5.13 and 6.86 10⁻⁵ Einstein min⁻¹ L⁻¹ with 1, 2, 3 and 4 lamps switched on, were obtained (Rivas et al.,

2015). Moreover, the intensity decreased to $3.65 \cdot 10^{-5} \text{ Einstein min}^{-1} \text{ L}^{-1}$ when the aluminum foil covering the internal wall was substituted by a black surface (4 lamps switched on).

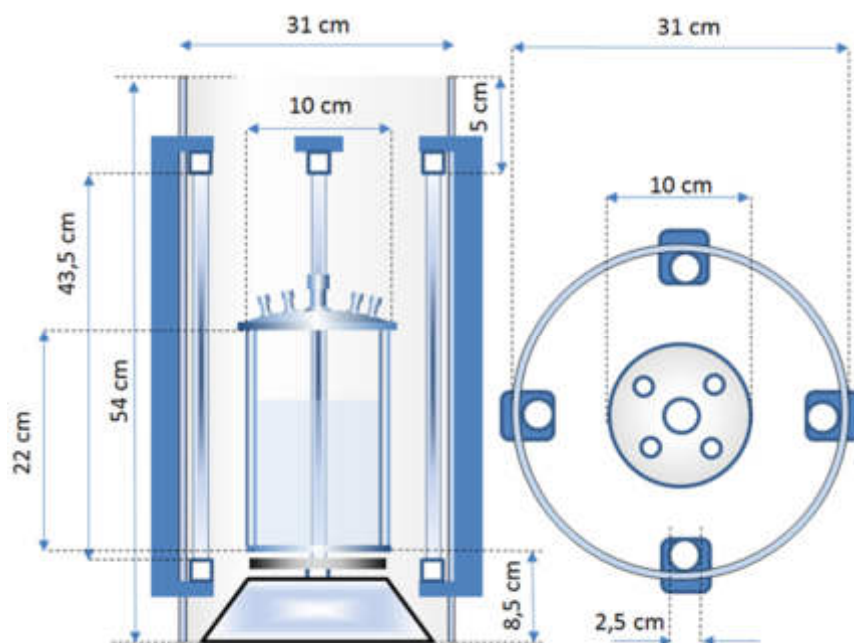


Figure 1. Frontal and top views of the photoreactor setup.

In all experiments 5 mg L^{-1} of initial tembotrione was used. This abnormally high concentration was used to be able to monitor TOC evolution. Homogeneous experiments of MPS oxidation were carried out with the lamps switched off, under stirring and control of temperature. Less than 10 mL of MPS was added from a high concentrated solution to start the reaction. Steadily samples were withdrawn from the reactor and quenched with $\text{Na}_2\text{S}_2\text{O}_3$ 0.5 M (10 μL per 10 mL of sample). When required, pH was controlled by NaOH or HCl addition. Heterogeneous photocatalytic experiments were carried out in the same way, in this case, in order to reach the tembotrione adsorption equilibria onto titanium dioxide (if any), each trial was preceded by 30 min of stirring under absence of radiation. Millex-HA filters (Millipore, $0.45 \mu\text{m}$) were used to remove the catalyst before analyses.

3. RESULTS AND DISCUSSION

3.1. Monopersulfate promoted experiments in the absence of light and photocatalyst

3.1.1. Influence of initial Oxone® concentration

A series of preliminary experiments was carried out to investigate the potential oxidation of tembotrione by monopersulfate as a sole oxidizing agent. The capability of monopersulfate as oxidant in the absence of any decomposition promoter has been reported previously by some authors (Rivas et al., 2012).

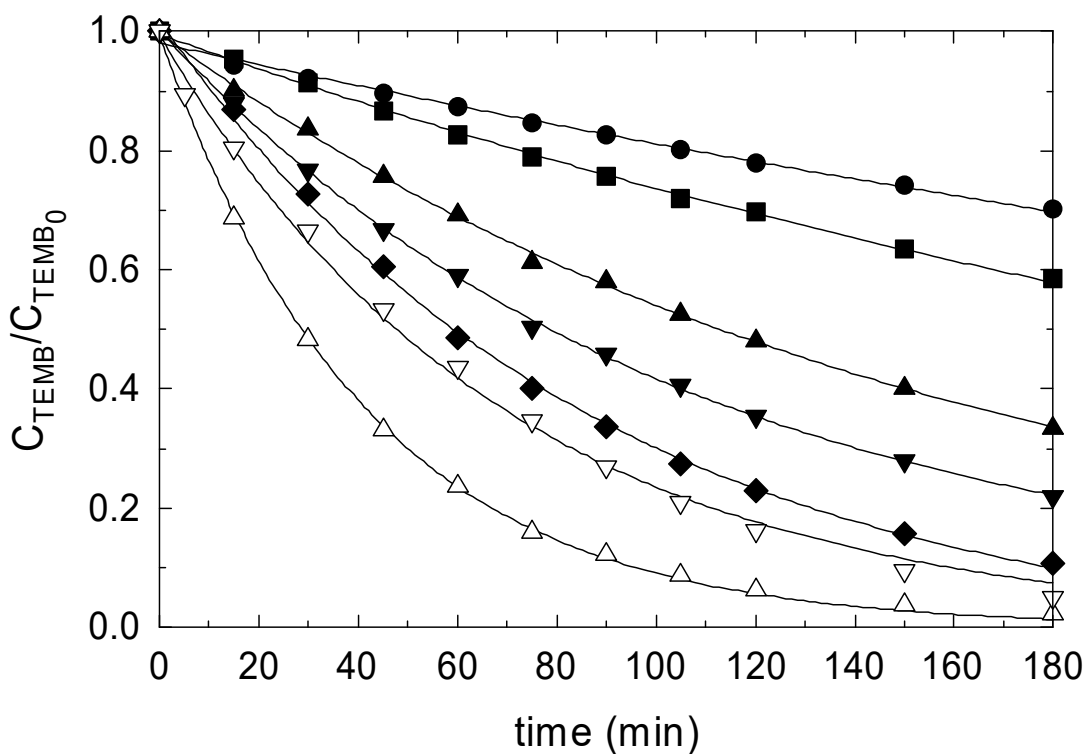


Figure 2. Oxone® oxidation of tembotrione. Influence of the initial Oxone® concentration. Experimental conditions: $T = 25^{\circ}\text{C}$; $V = 1.0\text{ L}$; $\text{pH} = 3.1$; $C_{\text{TEMB},0} = 5\text{ mg L}^{-1}$ (average value); $C_{\text{Oxone},0}\text{ (M}\cdot 10^4\text{)}$: \bullet , 1.05; \blacksquare , 2.52; \blacktriangle , 5.0; \blacktriangledown , 10.0; \blacklozenge , 25.1; ∇ , 50.0; Δ , 10.0 (in the presence of UVA light). Solid lines correspond to pseudofirst order kinetics fitting, $R^2 > 0.99$ in all cases.

Figure 2 shows the evolution of normalized tembotrione concentration in experiments conducted in the presence of initial Oxone® concentrations in the range $1.0\text{-}50\cdot 10^{-4}$ M. As inferred from the figure, tembotrione is eliminated at acceptable rates by apparently following exponential pseudofirst order kinetics. In these experiments, however, no TOC reduction was appreciated, suggesting the absence or insufficient generation of powerful free radicals species. Addition to double bonds is normally associated to direct attack of monopersulfate to organic molecules (Renganathan and Maruthamuthu, 1986). In the worst case, initial tembotrione concentration is at least 20 times lower than monopersulfate concentration. Accordingly, it can be assumed that Oxone® concentration will remain practically constant along the oxidation experiments. Also, as stated previously, monopersulfate likely adds to any tembotrione double bond in the molecule. Since this compound presents several positions of potential attack, a generic n-th order was assumed regarding Oxone® concentration. As a consequence, the following kinetic expression was assumed to describe the process:

$$-\frac{dC_{\text{TEMB}}}{dt} = k C_{\text{TEMB}} C_{\text{Oxone}}^n \quad (1)$$

Where k is a rate constant depending on temperature and pH. If Oxone® concentration remains constant:

$$-\frac{dC_{\text{TEMB}}}{dt} = k C_{\text{Oxone}_0}^n C_{\text{TEMB}} = k_{\text{Obs}} C_{\text{TEMB}} \quad (2)$$

After integration:

$$\ln \frac{C_{\text{TEMB}_0}}{C_{\text{TEMB}}} = k_{\text{Obs}} t \quad (3)$$

Values of k_{Obs} were obtained after plotting the left side member in equation 3 versus time, leading to values of 0.113 ± 0.002 , 0.179 ± 0.005 , 0.364 ± 0.012 , 0.506 ± 0.015 ,

0.754±0.014, 1.278±0.02 h⁻¹ in experiments completed in the presence of 1.05, 2.52, 5.0, 10.0, 25.1, and 50.0 10⁻⁴ M in Oxone® initial concentration, respectively.

The order regarding Oxone® concentration could be obtained after applying natural logarithms to k_{Obs}:

$$\begin{aligned} k_{\text{Obs}} &= k \cdot C_{\text{Oxone}_0}^n \\ \ln(k_{\text{Obs}}) &= \ln(k) + n \ln(C_{\text{Oxone}_0}) \end{aligned} \quad (4)$$

An adequate plot of Equation 4 led to a value of n = 0.62±0.03 (≈ 2/3) and k = 22.2±1.43 M^{-0.62} h⁻¹ (R² = 0.99) at pH 3.1.

3.1.2. Influence of temperature

Temperature influence was investigated in the interval 25-60°C. Experiments were conducted in the presence of 10⁻³ M in Oxone®. Figure 3 shows the results obtained. Once again pseudofirst order kinetics regarding tembotrione concentration could acceptably describe the process. In this case, calculated k_{Obs} values were 0.506±0.015, 1.264±0.04, 2.293±0.08, and 4.290±0.06 h⁻¹, corresponding to experiments completed at 25, 40, 50, and 60°C, respectively.

Although heat could activate the decomposition of MPS into radicals, monopersulfate is poorly activated at temperatures below 80°C (Yang at al., 2010). Accordingly, any effect observed by an increase in temperature will only be related to changes in the value of the direct rate constant.

Assuming Arrhenius behavior in the observed rate constant:

$$\begin{aligned} k_{\text{Obs}} &= A \cdot C_{\text{Oxone}_0}^n \cdot e^{-\frac{E_A}{RT}} \\ \ln(k_{\text{Obs}}) &= \ln(A \cdot C_{\text{Oxone}_0}^n) - \frac{E_A}{R} \frac{1}{T} \end{aligned} \quad (5)$$

Where R is the universal gas constant, E_A is the activation energy of the process and A , the pre-exponential factor.

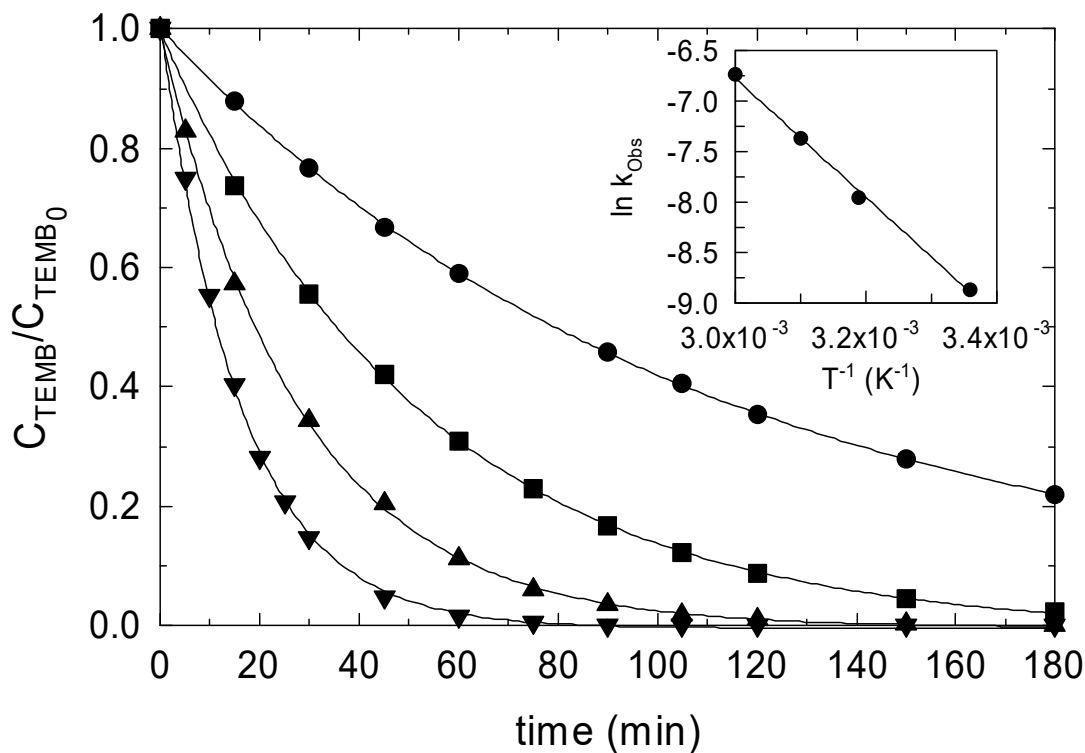


Figure 3. Oxone® oxidation of tembotrione. Influence of temperature. Experimental conditions: $C_{\text{Oxone},0} = 10.0 \cdot 10^4 \text{ M}$; $V = 1.0 \text{ L}$; $\text{pH} = 3.1$; $C_{\text{TEMB},0} = 5 \text{ mg L}^{-1}$ (average value); $T \text{ (}^\circ\text{C)}$: \bullet , 25; \blacksquare , 40; \blacktriangle , 50; \blacktriangledown , 60. (inset: Arrhenius plot). Solid lines correspond to pseudofirst order kinetics fitting, $R^2 \approx 0.999$ in all cases.

A plot of equation 5 is shown in the inset of Figure 3. From this plot, the activation energy of the process was calculated to be $50.1 \pm 0.1 \text{ kJ mol}^{-1}$.

Again, no significant TOC reduction was experienced regardless of the temperature used.

3.1.3. Influence of pH

pH is an important parameter in monopersulfate oxidation mediated processes (Rivas et al., 2013). This aspect was assessed by completing an experimental series at different pHs in the range 3-12. Figure 4 shows the results obtained.

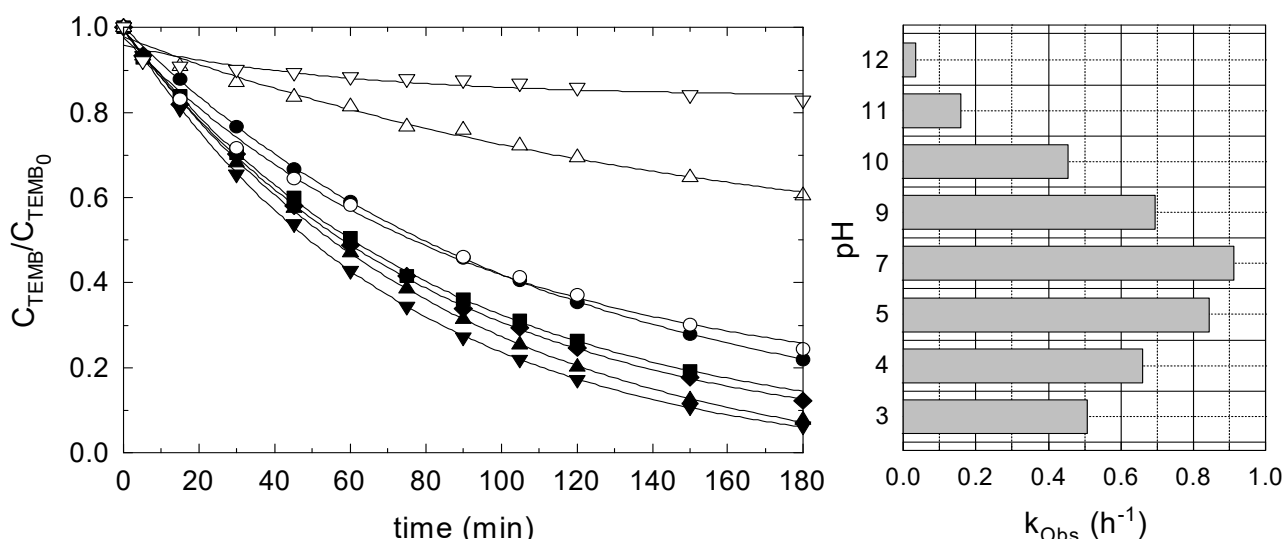


Figure 4. Oxone® oxidation of tembotrione. Influence of pH. Experimental conditions: $T = 25\text{ }^{\circ}\text{C}$; $C_{\text{Oxone},0} = 10^{-3}\text{ M}$; $V = 1.0\text{ L}$; $C_{\text{TEMB},0} = 5\text{ mg L}^{-1}$ (average value); pH: ●, 3.1; ■, 4.0; ▲, 5.0; ▼, 7.0; ◆, 9.0; ○, 10.0; △, 11.0; ▽, 12.0. (Right figure: observed rate constant as a function of pH). Solid lines correspond to pseudofirst order kinetics fitting, $R^2 > 0.99$ in all cases.

Figure 4 reveals an optimum in pH around 7.0. Two effects could be considered to explain these results. Hence, monopersulfate has a second acid dissociation pK_a of roughly 9.4 while tembotrione presents a pK_a of 3.2. It seems that the anionic form of tembotrione is more reactive than the molecular form, that is, increasing the pH above 3 up to circumneutral conditions favors the process since the oxidant remains as HSO_5^- . Contrarily, if pH is increased above 7-8, monopersulfate dissociates and the

predominant species is SO_5^{2-} , which, apparently, reacts with the ionic form of tembotrione at a lower rate than the protonated form. No mineralization of the parent compound was observed no matter the working pH used.

As stated previously, no TOC reduction could be achieved by using monopersulfate as the only oxidant agent. In an attempt to improve the process, UVA light was applied to the reaction media (see Figure 2). As seen in Figure 2, tembotrione depletion was slightly improved if compared to the run conducted in the dark under similar conditions. This improvement could be associated to partial Oxone® decomposition due to UVA light absorption (not probable because Oxone® does not absorb at 365 nm) or the generation of some intermediates acting as sensitizers of the photolysis (tembotrione does not absorb UVA light). Some mechanistic aspects will be discussed later. In any case, no mineralization of the herbicide could be detected.

3.2. Oxone® promoted tembotrione photocatalysis in the presence of TiO_2

In a final effort to increase the efficacy of the oxidation system in terms of tembotrione abatement rate and mineralization extent, titania powder was added to the reaction media. TiO_2 in the absence of oxone would constitute the conventional photocatalytic process, however, if MPS is added, this promoter could also be decomposed onto the titania surface. This latter aspect was first studied.

3.2.1. Oxone® photocatalysis

The combination of light, titania and an inorganic peroxide has been proven to be an efficient technology to deal with recalcitrant substances. Hence, several works report the benefits of adding hydrogen peroxide, monopersulfate or persulfate in photocatalytic processes carried out with UVC lamps (Gimeno et al., 2007). However, not many works have been focused on the use of other UV sources such as black light or visible radiation. Apparently, the advantages of adding inorganic peroxides to a photolytic

process come from the decomposition of the promoter to give powerful radical species. Accordingly, some preliminary studies were conducted to ascertain the capacity of the combination of UVA and TiO₂ to decompose monopersulfate.

A first experimental series was conducted with the system Oxone®/TiO₂/UVA at different titania initial concentrations by maintaining the rest of operating variables constant. Figure 5 shows the normalized monopersulfate concentration with time.

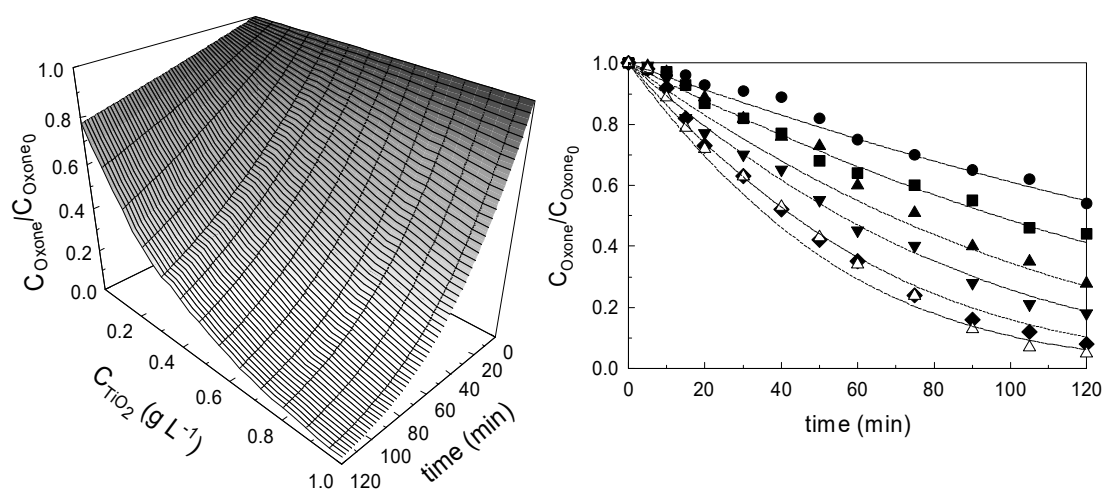


Figure 5. Photocatalytic Oxone® decomposition in the presence of black light. Influence of titania concentration. Experimental conditions: $V = 1.0 \text{ L}$, $T = 25^\circ\text{C}$, $\text{pH} = 3.1$, $C_{\text{Oxone},0} = 1.8 \cdot 10^{-3} \text{ M}$, $C_{\text{TiO}_2} (\text{g L}^{-1})$: ●, 0.05; ■, 0.1; ▲, 0.2; ▼, 0.3; ◆, 0.5; △, 0.7. Dashed lines correspond to model calculations with $k_{\text{obs, Oxone}} = 9 \cdot 10^{-5} \text{ mol L}^{-0.5} \text{ g}^{-0.5} \text{ min}^{-1}$ and $K_{\text{ads}} = 375 \text{ M}^{-1}$. (left figure = 3D theoretical concentration profiles as a function of catalyst concentration).

As observed in Figure 5, titania concentration exerts a positive effect up to values of 0.5 g L^{-1} , reaching thereafter a plateau for higher TiO₂ amounts. The optimum concentration does not coincide with the optimum found in tembotrione photocatalysis, the reason is unclear. Likely, adsorption of Oxone® onto the catalyst proceeds to a lesser extent than

tembotrione, accordingly, agglomeration of particles is not a significant drawback. In any case, besides of geometry and reactor configuration, the bibliography suggests that the optimum in titania concentration highly depends on the nature of the substance to be oxidized.

If the initial concentration of Oxone® is varied, the results discard the development of first order kinetics. Figure 6 shows the evolution profiles of Oxone® in this experimental series.

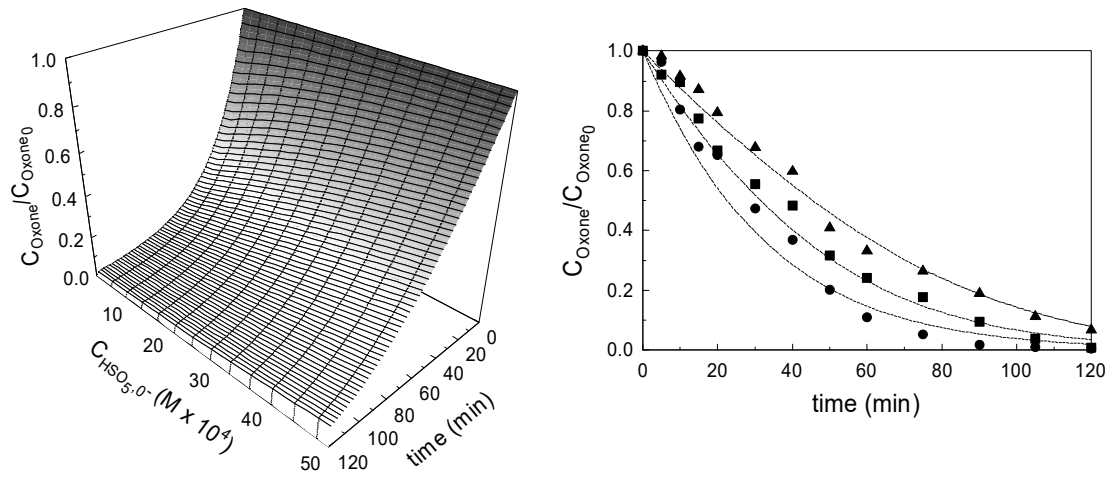


Figure 6. Photocatalytic Oxone® decomposition in the presence of black light. Influence of initial Oxone® concentration. Experimental conditions: $V = 1.0 \text{ L}$, $T = 25^\circ\text{C}$, $\text{pH} = 3.1$, $C_{\text{TiO}_2} = 1.0 \text{ g L}^{-1}$, $C_{\text{Oxone},0} \text{ (M)}$: ●, $2.0 \cdot 10^{-4}$; ■, $1.0 \cdot 10^{-3}$; ▲, $2.0 \cdot 10^{-3}$. Dashed lines correspond to model calculations with $k_{\text{obs,Oxone}} = 9 \cdot 10^{-5} \text{ mol L}^{-0.5} \text{ g}^{-0.5} \text{ min}^{-1}$ and $K_{\text{ads}} = 375 \text{ M}^{-1}$. (left figure = 3D theoretical concentration profiles as a function of monopersulfate concentration).

Langmuir equation is a common kinetic expression applied in photocatalytic processes. Depending on substrate concentration, Langmuir can lead to zero or first order kinetics. None of the aforementioned reaction orders can be applied to results in Figure 6. Hence, conversion decreases as initial Oxone® concentration is increased discarding, therefore,

first order kinetics. No straight lines are obtained, ruling out, in this case, zero order kinetics. As a consequence, a generic expression was adopted to describe the process:

$$\frac{dC_{\text{HSO}_5^-}}{dt} = k_{\text{oxone}} C_{\text{HSO}_5^-}^{\alpha} - C_{\text{TiO}_2}^{\beta} C_{\text{H}^+}^{\gamma} \quad (6)$$

Where α , β , and γ are the reaction order regarding monopersulfate, titania and protons concentration, respectively and k_{Oxone} is the rate constant of the process. If Equation 6 is applied to experiments in Figure 6:

$$\frac{dC_{\text{HSO}_5^-}}{dt} = \left[k_{\text{oxone}} C_{\text{TiO}_2}^{\beta} C_{\text{H}^+}^{\gamma} \right] C_{\text{HSO}_5^-}^{\alpha} = K_{\beta\gamma} C_{\text{HSO}_5^-}^{\alpha} \quad (7)$$

Applying the differential method in kinetic analysis:

$$\ln \left(\frac{dC_{\text{HSO}_5^-}}{dt} \right) = \ln(K_{\beta\gamma}) + \alpha \ln C_{\text{HSO}_5^-} \quad (8)$$

A plot of the natural logarithm corresponding to monopersulfate depletion rate versus the monopersulfate concentration natural logarithm led to a straight line ($R^2 = 0.95$) of slope 0.62 ± 0.02 . The order regarding monopersulfate concentration is located in the interval 0-1, i.e. in the middle of the limiting values in Langmuir kinetics.

Analogously, if experiments in Figure 5 are considered, taking into account the definition of $K_{\beta\gamma}$ and the value of $\alpha = 0.62$:

$$\ln(K_{\beta\gamma}) = \beta \ln(C_{\text{TiO}_2}) + \ln(k_{\text{Oxone}} C_{\text{H}^+}^{\gamma}) \quad (9)$$

Different values of $K_{\beta\gamma}$ could be obtained from Figure 5, allowing, thereafter, the adequate representation of Equation 9. The straight line obtained ($R^2 > 0.99$) led to a value of $\beta = 0.48 \pm 0.02$. This reaction order applies to experiments shown in Figure 5.

Hence, if values of TiO_2 concentration are above $0.5\text{--}0.7\text{ g L}^{-1}$, no influence of this parameter was observed (results not shown) and β is expected to be close to zero.

A final experimental series was conducted in the presence of well-known free radicals inhibitors. For instance, tert-butanol (t-BuOH) and methanol (MeOH) react with hydroxyl and sulfate radicals with rate constant values of $6 \cdot 10^8$ (Wolfenden and Willson, 1982) and $4 \cdot 10^5\text{ M}^{-1}\text{ s}^{-1}$ (Eibenberger et al., 1978), respectively for the first one, and $9.7 \cdot 10^8$ (Buxton et al., 1988) and $3.2 \cdot 10^6\text{ M}^{-1}\text{ s}^{-1}$ (Eibenberger et al., 1978) corresponding to the second alcohol. Bicarbonates were also used, although in this case both rate constants are similar, $8.5 \cdot 10^6\text{ M}^{-1}\text{ s}^{-1}$ (Buxton and Elliot, 1986) and $9.1 \cdot 10^6\text{ M}^{-1}\text{ s}^{-1}$ (Dogliotti and Hayon, 1967), respectively. Figure 7 illustrates the results obtained.

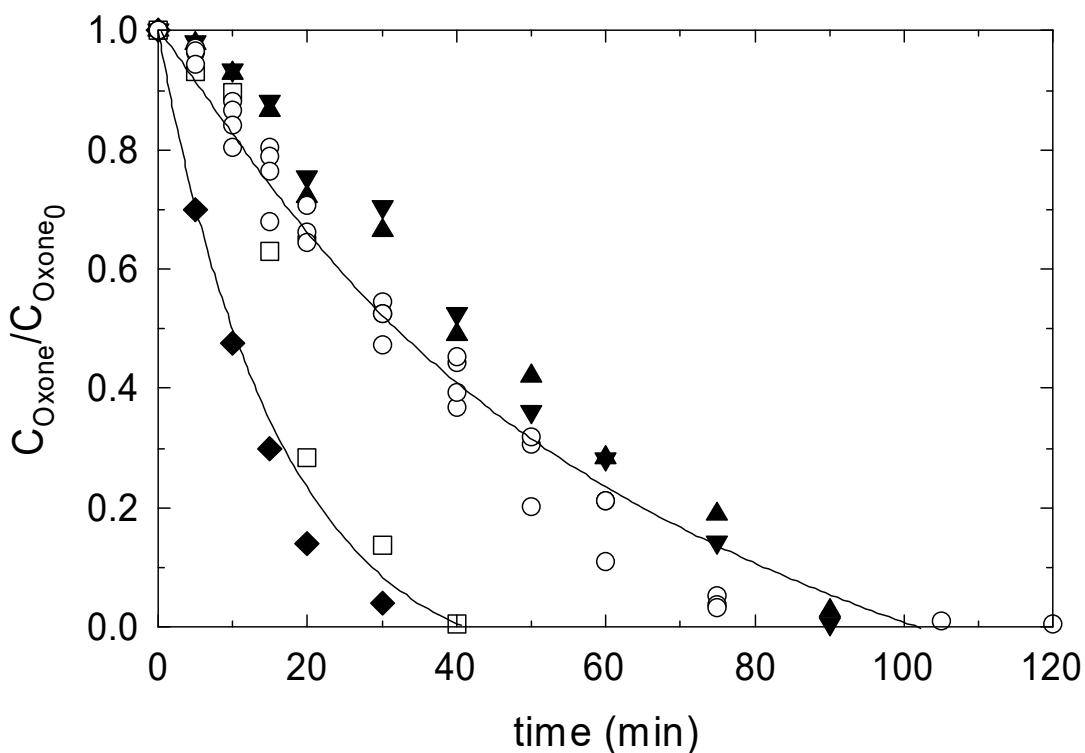
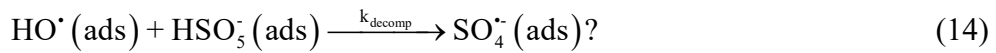


Figure 7. Photocatalytic Oxone® decomposition in the presence of black light. Influence of free radical scavengers. Experimental conditions: $V = 1.0\text{ L}$, $T = 25^\circ\text{C}$, pH

= 3.1, $C_{\text{TiO}_2} = 1.0 \text{ g L}^{-1}$, $C_{\text{Oxone},0} = 3.2 \cdot 10^{-4} \text{ M}$: ○, No scavengers; □, No scavengers pH = 12; ♦, $\text{HCO}_3^- \cdot 10^{-2} \text{ M}$ (pH = 10.6); ▼, MeOH 10^{-2} M ; ▲, t-BuOH 10^{-2} M .

Figure 7 reveals the negligible influence of MeOH and t-BuOH. Additionally, the presence of carbonates shifts the pH media to alkaline conditions (pH≈11) where monopersulfate is completely dissociated. Consequently, the effect of carbonates must be studied under similar conditions. An experiment carried out at pH 12 in the absence of carbonates again corroborated the null influence of radical scavengers addition. According to the previous results, the development of a surface reaction is suggested, ruling out the presence of free radicals in solution.

By considering the previous hypothesis and the experimental results, the following mechanism was proposed:



Equation 10 is the hole-electron generation stage which depends on light intensity, reactor geometry, catalyst concentration, radiation wavelength, etc. A general expression has been used in this study (Marugán et al., 2011):

$$r_g = \frac{\phi \text{ LVRPA}}{S_{\text{TiO}_2} C_{\text{TiO}_2}} = \frac{\zeta}{C_{\text{TiO}_2}} \quad (15)$$

ϕ is the quantum yield, LVRPA is the local volumetric rate of photon absorption and S_{TiO_2} and C_{TiO_2} stand for the specific surface and concentration of titanium dioxide.

If steady state conditions are applied to electron and hole concentrations:

$$C_{e^-} = \frac{r_g}{k_T C_{h^+} + k_{\text{trapping}} C_{\text{O}_2}} \quad (16)$$

$$C_{h^+} = \frac{r_g}{k_T C_{e^-} + k_{\text{hole}} C_{\text{H}_2\text{O}}} \quad (17)$$

Substituting 16 in 17:

$$C_{h^+} = k_1 \left(-1 + \sqrt{1 + \frac{\lambda}{C_{\text{TiO}_2}}} \right) \quad (18)$$

where:

$$k_1 = \frac{k_{\text{trapping}} C_{\text{O}_2}}{2k_T} \quad (19)$$

and

$$\lambda = \frac{4k_T \zeta}{k_{\text{trapping}} k_{h^+} C_{\text{O}_2}} \quad (20)$$

Monopersulfate adsorption is defined through the equilibrium:

$$K_{\text{ads}} = \frac{C_{\text{HSO}_3^-(\text{ads})}}{C_{\text{HSO}_3^-} C_{\text{empty sites}}^{\text{TiO}_2}} \quad (21)$$

The total number of adsorption sites on TiO_2 surface is the sum of “empty sites” plus those already occupied by monopersulfate. Additionally, the number of adsorption sites is proportional to titania concentration, mathematically:

$$\theta C_{\text{TiO}_2} = C_{\text{HSO}_3^-} + \frac{C_{\text{HSO}_3^-(\text{ads})}}{C_{\text{HSO}_3^-} K_{\text{ads}}} \quad (22)$$

Finally, monopersulfate removal rate is expressed as:

$$-\frac{dC_{\text{HSO}_5}}{dt} = k_{\text{decomp}} C_{\text{HSO}_5(\text{ads})} C_{\text{HO}^\bullet} = k_{\text{decomp}} \theta C_{\text{TiO}_2} \frac{C_{\text{HSO}_5} K_{\text{ads}}}{1 + C_{\text{HSO}_5} K_{\text{ads}}} k_{\text{hole}} C_{\text{h}^\bullet} C_{\text{H}_2\text{O}} \quad (23)$$

$$-\frac{dC_{\text{HSO}_5}}{dt} = k_{\text{decomp}} \theta C_{\text{TiO}_2} \frac{C_{\text{HSO}_5} K_{\text{ads}}}{1 + C_{\text{HSO}_5} K_{\text{ads}}} k_{\text{hole}} k_1 C_{\text{H}_2\text{O}} \left(-1 + \sqrt{1 + \frac{\lambda}{C_{\text{TiO}_2}}} \right) \quad (24)$$

In those cases where radiation intensity is sufficiently high, it follows that $\frac{\lambda}{C_{\text{TiO}_2}} \gg 1$

leading to:

$$-\frac{dC_{\text{HSO}_5}}{dt} = k_{\text{obs, Oxone}} \sqrt{C_{\text{TiO}_2}} \frac{C_{\text{HSO}_5} K_{\text{ads}}}{1 + C_{\text{HSO}_5} K_{\text{ads}}} \quad (25)$$

Equation 25 corroborates the experimental reactions orders experimentally found with respect to titania and monopersulfate concentrations. This kinetic expression was used in a fitting process to estimate the values of the unknown $k_{\text{obs, Oxone}}$ and K_{ads} . Values of $k_{\text{obs, Oxone}}$ and K_{ads} of $9 \cdot 10^{-5} \text{ mol L}^{-0.5} \text{ g}^{-0.5} \text{ min}^{-1}$ and 375 M^{-1} , respectively, were capable of acceptably simulate the influence of both initial Oxone® and titania concentrations (see model calculations in Figures 5 and 6).

Once the capability of the UVA and TiO_2 system to decompose Oxone® has been demonstrated, it would be necessary that reaction 14 led to formation of active oxidizing species on titania surface. Accordingly, the photocatalysis of tembotrione was conducted in the presence of Oxone® as a promoter.

3.2.2. Oxone® promoted tembotrione photocatalysis

In an attempt to accelerate the parent compound removal and simultaneously increase mineralization, some experiments were conducted in the presence of Oxone® and

Degussa P25 titania applying UVA light at 365 nm. For comparison purposes, some non-promoted experiments were also carried out.

Figure 8 shows the evolution of the normalized tembotrione concentration in experiments conducted in the presence of titania at two different pHs. As observed, the process is significantly improved both in terms of tembotrione abatement rate and mineralization extent if compared to the application of Oxone® as the unique oxidant.

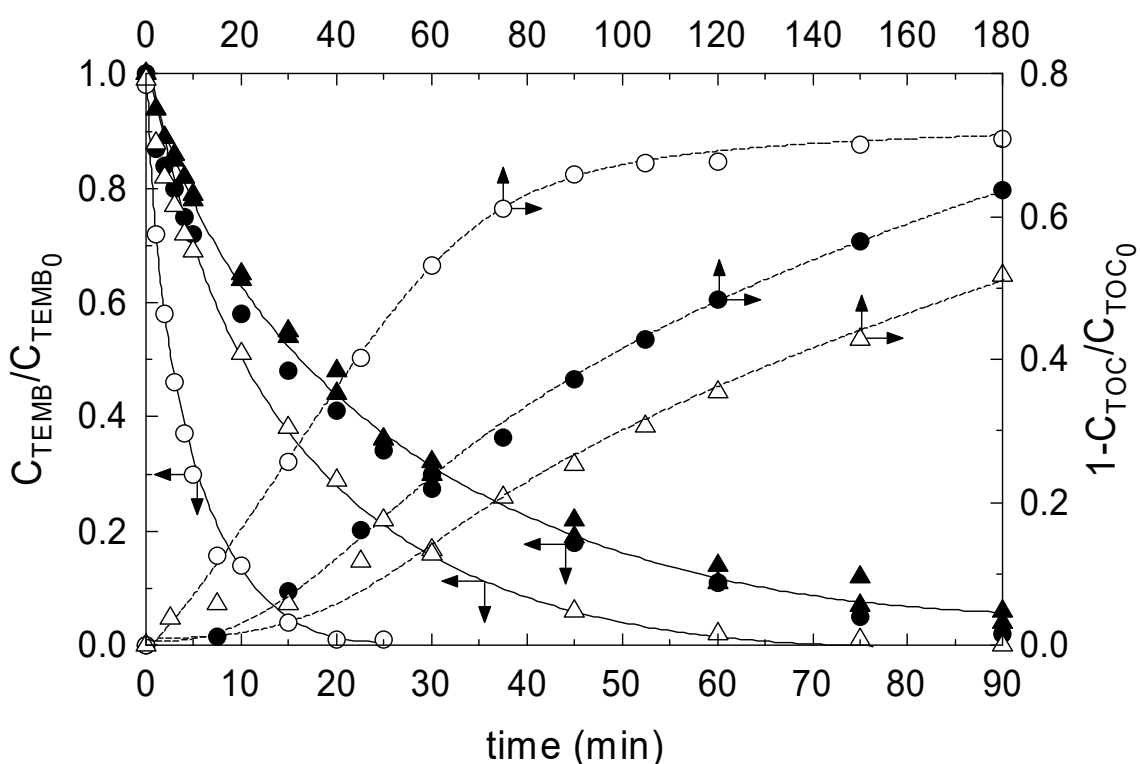


Figure 8. Photocatalysis of tembotrione in the presence of titania P-25. Influence of Oxone® addition at different pHs. Experimental conditions: $T = 25^{\circ}\text{C}$; $V = 1.0 \text{ L}$; $\text{pH} = 5.1$; $C_{\text{TEMB},0} = 5 \text{ mg L}^{-1}$ (average value); $C_{\text{TiO}_2} = 0.05 \text{ g L}^{-1}$. Symbols: ●, pH 3.1 and $C_{\text{Oxone},0} = 0.0 \text{ M}$; ○, pH 3.1 and $C_{\text{Oxone},0} = 10^{-4} \text{ M}$; ▲, pH 7.0 and $C_{\text{Oxone},0} = 0.0 \text{ M}$; △, pH 7.0 and $C_{\text{Oxone},0} = 10^{-4} \text{ M}$. Solid lines correspond to pseudofirst order kinetics fitting, $R^2 > 0.99$ in all cases.

When pH is not adjusted, the non-promoted photocatalysis of tembotrione leads to total parent compound abatement in roughly 90 min while if 10^{-4} M of Oxone® is added, this time is reduced to 20 min. pH does not exert a significant effect in tembotrione abatement when monopersulfate is not added to the reaction media, however some inhibition was observed in Oxone® promoted experiments when increasing the pH from 3.1 to 7. pH effect is associated to several parameters such as reagents pK_a and also the point of zero charge of titania which influences the adsorption extent.

The extent of synergism ($\Lambda_{\text{Synergism}}$) reached during tembotrione oxidation could be calculated as follows:

$$\Lambda_{\text{Synergism}} (\%) = \frac{k_{\text{OxonePhotoCat}} - (k_{\text{PhotoCat}} - k_{\text{Oxone}})}{k_{\text{OxonePhotoCat}}} \times 100 \quad (26)$$

where $k_{\text{OxonePhotoCat}}$, k_{PhotoCat} and k_{Oxone} represent the empirical pseudofirst order rate constant corresponding to photocatalytic oxidation promoted with Oxone®, without Oxone® and the direct reaction with Oxone®, respectively. Table 1 shows the results of synergism. Hence, promoted photocatalytic oxidation cannot be explained as the sum of photocatalytic and direct oxidation processes, reaching higher synergism values for tembotrione at acidic pH.

Table 1. Experimental pseudofirst order rate constant of tembotrione and TOC removal obtained from Figure 8

	Tembotrione				TOC			
	$k_{\text{OxonePhotoCat}}$ (R^2)	k_{PhotoCat} (R^2)	k_{Oxone} (R^2)	$\Lambda_{\text{Synergism}}$ (%)	$k_{\text{OxonePhotoCat}}$ (R^2)	k_{PhotoCat} (R^2)	k_{Oxone} (R^2)	$\Lambda_{\text{Synergism}}$ (%)
Uncontrolled	12.69	2.33	0.11	80.8	0.78	0.36	0	53.8
pH	(0.994)	(0.984)	(0.994)		(0.996)	(0.996)		
pH=7	3.69	1.82	0.22*	44.7	0.25	0	0	-
	(0.999)	(0.983)			(0.992)			

*Obtained theoretically from equation (4) knowing k_{Obs} at pH=7 and 10^{-3} M of Oxone®

It is also noteworthy to highlight the mineralization extent achieved. A maximum of roughly 70% after three hours of treatment was experienced when 0.05 g L⁻¹ of titania were used in the presence of Oxone® with no pH adjustment. Once again, a synergistic effect is appreciated in TOC removal (see Table 1).

In this section some experiments were conducted in the presence of free radical scavengers (results not shown) at a high concentration of Oxone® (10⁻³ M) in order to prove their inhibitory effect if any. Contrarily to Oxone® photocatalysis, partial inhibition of the process was experienced at pH=7 suggesting the presence of radicals in solution. Methanol showed a higher scavenging capacity than tert-butanol. If a sufficiently high scavenger concentration is used (0.01 M), both alcohols lead to similar results, reducing the pseudofirst order reaction rate constant from roughly 16 h⁻¹ to 6.3 h⁻¹.

3.2.3. Tembotrione photocatalysis in the presence of Oxone®. Experimental design

A final effort was made to optimize the promoted photocatalytic process by completing a Plackett-Burman experimental design (ED) with three factors and two center points. The three factors were the initial concentrations of Oxone® and herbicide concentration plus the amount of catalyst added to the reaction media. Although pH exerts a high influence in the process, in order to reduce the disadvantages associated to a pH adjusting step in a real application, this parameter has not been considered in the experimental design.

Table 2 shows the factor values of the ED. The observed pseudo first order rate constant in tembotrione was considered as the response of the process.

Table 2. Plackett-Burman experimental design and responses

Experiment	C _{TiO2} (g L ⁻¹)	C _{Oxone} ·10 ⁴ (M)	C _{TEMB,0} (mg L ⁻¹)	k _{TEMB} (min ⁻¹)	k _{TOC} ·10 ² (min ⁻¹)	k _{Oxone} ·10 ² (min ⁻¹)
1	0.05	13	4.65	0.23	1.07	0.23
2	0.50	0.083	1.23	0.08	0.46	1.68
3	0.05	0.083	1.22	0.20	1.22	2.03
4	0.10	1.0	2.42	0.23	1.02	1.83
5	0.10	1.1	2.43	0.23	0.64	1.37
6	0.50	13	1.29	0.79	0.68	0.70
7	0.05	12	4.60	0.23	0.81	0.17
8	0.50	0.083	5.12	0.04	0.63	0.59
9	0.50	14	4.59	0.25	0.64	0.46
10	0.05	0.14	5.11	0.06	0.44	1.01
11	0.05	0.11	1.27	0.29	1.44	1.54
12	0.50	0.13	3.66	0.04	0.18	1.11
13	0.05	12	0.88	0.98	1.61	0.79
14	0.50	13	0.88	1.01	1.05	0.45

The regression of the data was completed by codifying the values of the factors between -1 and 1 corresponding to the minimum and maximum values used. A freeware Excel addin was used in the process.

By considering a linear plus interaction regression, the best output of the tembotrione abatement rate constant and the corresponding ANOVA analysis is shown in Table 3.

Table 3. Modelling of tembotrione abatement and mineralization in the Oxone® promoted photocatalysis system. $k_{TEMB}^{-1} = b_0 + b_1 \cdot C_{TiO2} + b_2 \cdot C_{Oxone} + b_3 \cdot C_{TEMB} + b_4 \cdot C_{TiO2} \cdot C_{Oxone} + b_5 \cdot C_{Oxone} \cdot C_{TEMB}$

	Model parameters (1/k _{TEMB})	Model parameters p-value·10 ²	ANOVA analysis	Value
b₀	7.853	0.002	R²	0.941
b₁	2.575	1.277	R_{adj}	0.905
b₂	-5.876	0.022	Durbin Watson d	2.06

b₃	3.512	0.779	Sum of Squares (regression)	911
b₄	-2.782	0.973	Sum of Squares (residuals)	56.7
b₅	-2.650	2.877	F^{Signif} (Regression)	0.941

As inferred from Table 2, tembotrione abatement is acceptably modelled showing an R^2_{adj} of 0.905, i.e. all the terms in the model are significant. Under the operating conditions investigated, titania and tembotrione concentrations show a negative effect in the pseudofirst order rate constant while Oxone® exerts a positive influence. An optimum in titania concentration was experimentally observed in the proximity of 0.05 g L⁻¹, coinciding with theoretical calculations of the LVRPA (local volumetric rate of photon absorption) by means of Monte Carlo simulations (results not shown). The negative effect observed at higher titania concentrations is normally associated to a “shielding” effect, however, this aspect is at least controversial and is not substantiated by theoretical calculations. Likely, the negative effect observed is related to particle agglomeration leading to a lower surface exposed to radiation and tembotrione adsorption.

Figure 9 compares the values of k_{TEMB}^{-1} calculated and experimentally obtained. Also using the model parameters, some validation reactions completed at different titania concentrations and 10⁻⁴ M in Oxone® have been simulated and compared to model results. The simulation acceptably predicts the tembotrione removal profiles in runs not used in the experimental design. Some discrepancies were observed in the reaction completed with 0.05 g L⁻¹ in titania, however, given the complexity of the system, these differences can be assumed within the uncertainty of the process variables.

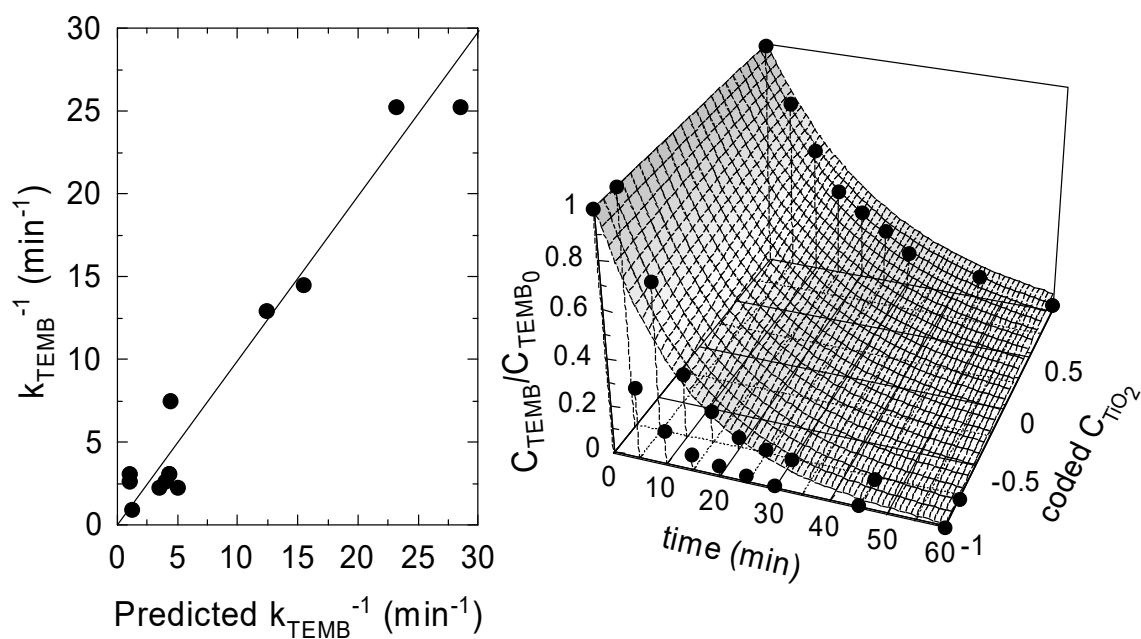


Figure 9. Oxone® promoted photocatalysis of tembotrione in the presence of titania P25. Left: comparison of experimental and model calculations. Right: Influence of titania concentration from model calculations. Experimental conditions: $T = 25\text{ }^{\circ}\text{C}$; $V = 1.0\text{ L}$; $\text{pH} = 3.1$; $C_{\text{Oxone},0} = 10^{-4}\text{ M}$, $C_{\text{TEMB},0} = 5\text{ mg L}^{-1}$ (●, experimental results at different titania concentrations).

4. CONCLUSIONS

Use of Oxone® seems to be a suitable alternative to oxidize organic aqueous contaminants. Direct tembotrione MPS oxidation follows 2/3 and first order in MPS and tembotrione concentrations, respectively. pH exerts an important effect since MPS and tembotrione pKa's do affect the process. 50.1 kJ mol^{-1} of activation energy was found to describe temperature influence on rate constant, according to Arrhenius definition.

MPS photocatalytic decomposition follows a Langmuir kinetic mechanism. Titania load exerts a positive effect until it reaches the optimum value of 0.5 g L^{-1} , afterwards it does

not accelerate MPS decomposition. Alcohol and carbonate scavengers have not shown significant effects.

MPS improves photocatalytic oxidation of tembotrione in both, parent compound and mineralization rate. The experimental design carried out shows that under the operating conditions investigated; titania and tembotrione concentrations show a negative effect in the pseudofirst order rate constant while Oxone® exerts a positive influence.

Acknowledgements

Authors thank economic support received from Gobierno de Extremadura and CICYT of Spain through Projects GRU10012 and CTQ2012-35789-C02-01, respectively. Mr. Rafael Rodríguez Solís also thanks Gobierno de Extremadura, Consejería de Empleo, Empresa e Innovación, and FSE Funds for his Ph.D. grant (PD12058).

References

Anipsitakis GP, Dionysiou DD, González MA. Cobalt-mediated activation of peroxymonosulphate and sulphate radical attack on phenolic compounds. Implications of chloride ions. *Environ Sci Technol* 2006;40:1000-1007.

Anipsitakis GP, Tufano TP, Dionysiou DD. Chemical and microbial decontamination of pool water using activated potassium peroxymonosulfate. *Water Res* 2008;48:2899-2910.

Anipsitakis GP, Stathatos E, Dionysiou DD. Heterogeneous Activation of Oxone Using Co_3O_4 . *J Phys Chem B* 109 2005;109:13052–13055.

Bensalah N, Khodary A, Abdel-Wahab A. Kinetic and mechanistic investigations of mesotrione degradation in aqueous medium by Fenton process. *J Hazard Mater* 2011;189:479-485.

Buxton GV, Elliot AJ. Rate constant for reaction of hydroxyl radicals with bicarbonate ions. *Int J Radiat Appl Instrum C Radiat Phys Chem* 1986;27:241-243.

Buxton GV, Greenstock CL, Helman WP, Ross AB. Critical review of rate constants for reactions of hydrated electrons, hydrogen atoms and hydroxyl radicals (radical dotOH/O⁻) in aqueous solution. *J Phys Chem Ref Data* 1988;17:513-886.

Calvayrac C, Bontemps N, Nougä-Bissoue A, Romdhane S, Coste CM, Cooper JF. Photolysis of tembotrione and its main by-products under extreme artificial conditions: Comparison with another β -triketone herbicide. *Sci Total Environ* 2013;452-453:227-232.

Commission implementing decision of 10 April 2012 allowing Member States to extend provisional authorisations granted for the new active substances amisulbrom, chlorantraniliprole, meptyldinocap, pinoxaden, silver thiosulfate and tembotrione. *Official Journal of the European Union* 2012;102:15-16.

Cong J, Wen G, Huang T, Deng L, Ma J. Study on enhanced ozonation degradation of para-chlorobenzoic acid by peroxymonosulfate in aqueous solution. *Chem Eng J* 2015;264:399-403.

Deng J, Shao Y, Gao N, Tan C, Zhou S, Hu X. CoFe₂O₄ magnetic nanoparticles as a highly active heterogeneous catalyst of oxone for the degradation of diclofenac in water. *J Hazard Mater* 2013;262:836-844.

Dogliotti L, Hayon E. Flash photolysis of per[oxydi]sulfate ions in aqueous solutions. The sulfate and ozonide radical anions. *J Phys Chem* 1967;71:2511-2516.

Eibenberger H, Steenken S, O'Neill P, Schulte-Frohlinde D. Pulse radiolysis and electron spin resonance studies concerning the reaction of $\text{SO}_4^{\bullet-}$ with alcohols and ethers in aqueous solution. *J Phys Chem* 1978;82:749-750.

Fernández J, Maruthamuthu PA, Kiwi J. Photobleaching and mineralization of Orange II by oxone and metal ions involving Fenton like chemistry under visible light. *J Photochem Photobiol A* 2004;161:185-192.

Fukushima M, Tatsumi T. Effect of Hydroxypropyl- β -cyclodextrin on the Degradation of Pentachlorophenol by Potassium Monopersulfate Catalyzed with Iron(III)-Porphyrin Complex. *Environ Sci Technol* 2005;39:9337-9342.

Gao YQ, Gao NY, Deng Y, Yin DQ, Zhang YS, Rong WL, Zhou SD, Heat-activated persulfate oxidation of sulfamethoxazole in water. *Desalination Water Treat* 2015;56:2225-2233.

Gimeno O, Carbajo M, López MJ, Melero JA, Beltrán FJ, Rivas FJ. Photocatalytic promoted oxidation of phenolic mixtures: An insight into the operating and mechanistic aspects. *Water Res* 2007;41:4672-4684.

Halle AT, Richard R. Simulated Solar Light Irradiation of Mesotrione in Natural Waters. *Environ Sci Technol* 2006;40:3842-3847.

Ji F, Li C, Deng L. Performance of CuO/Oxone system: Heterogeneous catalytic oxidation of phenol at ambient conditions. *Chem Eng J* 2011;178:239-243.

Jović M, Manojlović D, Stanković, Dojčinović B, Obradović B, Gašić U, Roglić G. Degradation of triketone herbicides, mesotrione and sulcotrione, using advanced oxidation processes. *J Hazard Mater* 2013;260:1092-1099.

Malato S, Blanco J, Richter C, Braun B, Maldonado MI. Enhancement of the rate of solar photocatalytic mineralization of organic pollutants by inorganic oxidizing species. *Appl Catal B: Environ* 1998;17:347-356.

Marugán J, Van Grieken R, Pablosa C, Satuf ML, Cassano AE, Alfano OM. Rigorous kinetic modelling with explicit radiation absorption effects of the photocatalytic inactivation of bacteria in water using suspended titanium dioxide. *Appl Catal B: Environ* 2011;102:404–416.

Miller JN, Miller JC, 2010. *Statistics and Chemometrics for Analytical Chemistry*, sixth ed. Pearson, Harlow.

Murati M, Oturan N, Aaron JJ, Dirany A, Tassin B, Zdravkovski, Oturan MA. Degradation and mineralization of sulcotrione and mesotrione in aqueous medium by the electro-Fenton process: a kinetic study. *Environ Sci Pollut Res* 2012;19:1563-1573.

Renganathan R, Maruthamuthu PJ. Kinetics and mechanism of oxidation of aromatic aldehydes by peroxomonosulfate. *Chem Soc Perkin Trans* 1986;11:285-289.

Rivas FJ, Gimeno O, Borralho T, Carbajo M. UV-C radiation based methods for aqueous metoprolol elimination. *J Hazard Mater* 2010;179:357-362.

Rivas FJ, Gimeno O, Borralho T. Aqueous pharmaceutical compounds removal by potassium monopersulfate. Uncatalyzed and catalyzed semicontinuous experiments. *Chem Eng J* 2012;192:326-333.

Rivas J, Solis RR, Gimeno O, Sagasti J. Photocatalytic elimination of aqueous 2-methyl-4-chlorophenoxyacetic acid in the presence of commercial and nitrogen-doped TiO₂. *Int J Environ Sci Technol* 2015;12:513-526.

Romero A, Santos A, Vicente F, González C. Diuron abatement using activated persulfate: Effect of pH, Fe(II) and oxidant dosage. *Chem Eng J* 2010;162:257-265.

Shukla PR, Wang S, Ang HM, Tadé MO. Photocatalytic oxidation of phenolic compounds using zinc oxide and sulfate radicals under artificial solar light. *Sep Purif Technol* 2010;70:338-344.

Su S, Guo W, Leng Y, Yi C, Ma Z. Heterogeneous activation of Oxone by $\text{Co}_x\text{Fe}_{3-x}\text{O}_4$ nanocatalysts for degradation of rhodamine B. *J Hazard Mater* 2013;244-245:736-742.

Sun J, Li X, Feng F, Tian X. Oxone/ Co^{2+} oxidation as an advanced oxidation process: Comparison with traditional Fenton oxidation for treatment of landfill leachate. *Water Res* 2009;43:4363-4369.

Sutton P, Richards C, L. Buren L, Glasgow L. Activity of mesotrione on resistant weeds in maize, *Pest Manag Sci* 2002;58:981-984.

Tarara G, Fliege R, Desmarteau D, Kley C, Peters B. Environmental fate of tembotrione. *Bayer Crop Sci J* 2009;62:63-78.

Tawk A, Deborde M, Labanowski J, Gallard H. Chlorination of the β -triketone herbicides tembotrione and sulcotrione: Kinetic and mechanistic study, transformation products identification and toxicity. *Water Res* 2015;76:132-142.

Transparency Market Research USA & Canada, Global Tembotrione Market to be Driven by Usage in Glyphosate-Resistant Weed Control. <http://www.transparencymarketresearch.com/article/global-tembotrione-market.htm>, 2015 (accessed 1.4.2016)

Trivella A, Stawinoga M, Dayan FE, Cantrell CL, Mazellier P, Richard C. Photolysis of natural β -triketonic herbicides in water. *Water Res* 2015;78:28-36.

Yang S, Wang P, Yang X, Shan L, Zhang W, Shao X, Niu R. Degradation efficiencies of azo dye Acid Orange 7 by the interaction of heat, UV and anions with common oxidants: Persulfate, peroxymonosulfate and hydrogen peroxide. *J Hazard Mater* 2010;179:552-558.

Wolfenden BS, Willson RL. Radical-cations as Reference Chromogens in kinetic Studies of One-electron Transfer Reactions: Pulse Radiolysis Studies of 2,2'-Azinobis-(3-ethylbenzthiazoline-6-sulphonate). *J Chem Soc Perkin Trans II* 1982:805-812.

Yao Y, Xu C, Qin J, Wei F, Rao M, Wang S. Synthesis of Magnetic Cobalt Nanoparticles Anchored on Graphene Nanosheets and Catalytic Decomposition of Orange I. *Ind Eng Chem Res* 2013;52:17341-17350.